iScience

CellPress
OPEN ACCESS

Article

Dynamic-tuning yeast storage carbohydrate improves the production of acetyl-CoA-derived chemicals

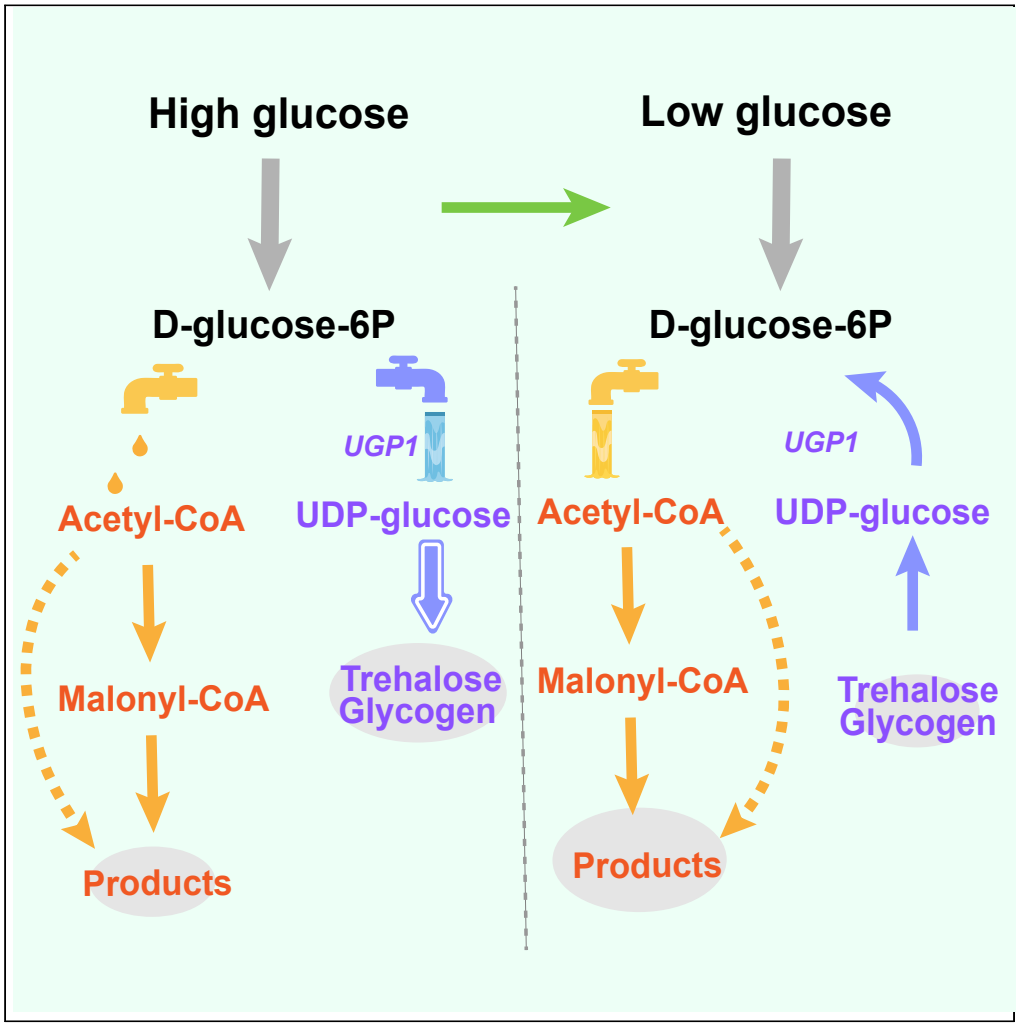

Chenxi Qiu, Huilin Tao, Yu Shen, Qingsheng Qi, Jin Hou

houjin@sdu.edu.cn

Highlights

Regulating the glycogen and trehalose accumulation affects the malonyl-CoA flux

Ugp1 improves the malonyl-CoA flux through dynamic-tuning storage carbohydrate

UGP1 overexpression also improves acetyl-CoA-derived chemicals

Qiu et al., iScience 26, 105817
January 20, 2023
https://doi.org/10.1016/j.isci.2022.105817

iScience

CellPress
OPEN ACCESS

Article

Dynamic-tuning yeast storage carbohydrate improves the production of acetyl-CoA-derived chemicals

Chenxi Qiu,[1,2] Huilin Tao,[1] Yu Shen,[1] Qingsheng Qi,[1] and Jin Hou[1,3,*]

SUMMARY

Acetyl-coenzyme A (Acetyl-CoA) and malonyl-coenzyme A (malonyl-CoA) are important precursors for producing various chemicals, and their availability affects the production of their downstream chemicals. Storage carbohydrates are considered important carbon and energy reservoirs. Herein, we find that regulating the storage carbohydrate synthesis improves metabolic fluxes toward malonyl-CoA. Interestingly, not only directly decreasing storage carbohydrate accumulation improved malonyl-CoA availability but also increasing the storage carbohydrate by *UGP1* overexpression enables an even higher production of acetyl-CoA- and malonyl-CoA-derived chemicals. We find that Ugp1p overexpression dynamically regulates the carbon flux to storage carbohydrate synthesis. In early exponential phases, Ugp1 overexpression causes more storage carbohydrate accumulation, while the carbon flux is then redirected toward acetyl-CoA and malonyl-CoA in later phases, thereby contributing to the synthesis of their derived products. Our study demonstrates the importance of storage carbohydrates rearrangement for the availability of acetyl-CoA and malonyl-CoA and therefore will facilitate the synthesis of their derived chemicals.

INTRODUCTION

Saccharomyces cerevisiae is a widely used microbial cell factory for producing biofuels, chemicals, and pharmaceuticals.[1–3] Acetyl-coenzyme A (acetyl-CoA) and malonyl-coenzyme A (malonyl-CoA) are important central metabolites in yeast and are involved in many cellular processes such as phospholipid synthesis as well as cellular regulation.[2,4,5] They also act as precursor molecules for a variety of products, including isoprenoids, polyketides, flavonoids, and platform chemicals. These chemicals can be used as biofuels,[6,7] cosmetics, pharmaceuticals,[8–11] nutraceutical ingredients,[12–14] bulk chemicals,[15–17] and so on (Figure 1A). Therefore, increasing intracellular levels of acetyl-CoA and malonyl-CoA is essential for improving the production of a range of high value-added compounds.

In our previous study, we isolated strains with improved malonyl-CoA synthesis using biosensor-coupled *in vivo* mutagenesis.[18] Through whole-genome sequencing and transcriptome analysis, we found that reducing lysine and arginine synthesis and carbohydrate storage synthesis can improve malonyl-CoA availability. This demonstrates that weakening the carbon flux to other competitive metabolic pathways (such as glycogen or lysine and arginine) can improve malonyl-CoA synthesis. Consistent with this, Cardenas et al. also showed that the deletion of *GSY1* and *GSY2*, which encode glycogen synthase paralogues, increases the production of triacetic acid lactone (TAL), a chemical derived from malonyl-CoA.[19]

In yeast, glycogen and trehalose are representative storage carbohydrates. They play important roles in energy storage, glycolytic flux control, and protecting cells from stresses.[20] Reducing its flux can redirect the flux to glycolysis, thereby improving acetyl-CoA synthesis. In this study, we further investigated the genomic sequencing data and identified several new targets involved in carbohydrate storage that can enhance malonyl-CoA availability. Surprisingly, in addition to reducing glycogen synthesis, we found that increasing storage carbohydrate accumulation by *UGP1* overexpression can also boost malonyl-CoA synthesis. The increased range is even higher than that obtained by directly reducing storage carbohydrate accumulation. Ugp1, a UDP-glucose pyrophosphorylase, which catalyzes the reversible formation of UDP-glucose, is considered to be a crucial enzyme in carbohydrate metabolism.[21] Its catalyzed product UDP-glucose acts as a glucosyl donor and is involved in multiple cellular processes, including

[1]State Key Laboratory of Microbial Technology, Shandong University, Binhai Road 72, Qingdao, Shandong 266237, P. R. China

[2]Present address: College of Food and Biological Engineering, Henan University of Animal Husbandry and Economy, Zhengzhou 450000, P. R. China

[3]Lead contact

*Correspondence: houjin@sdu.edu.cn

https://doi.org/10.1016/j.isci.2022.105817

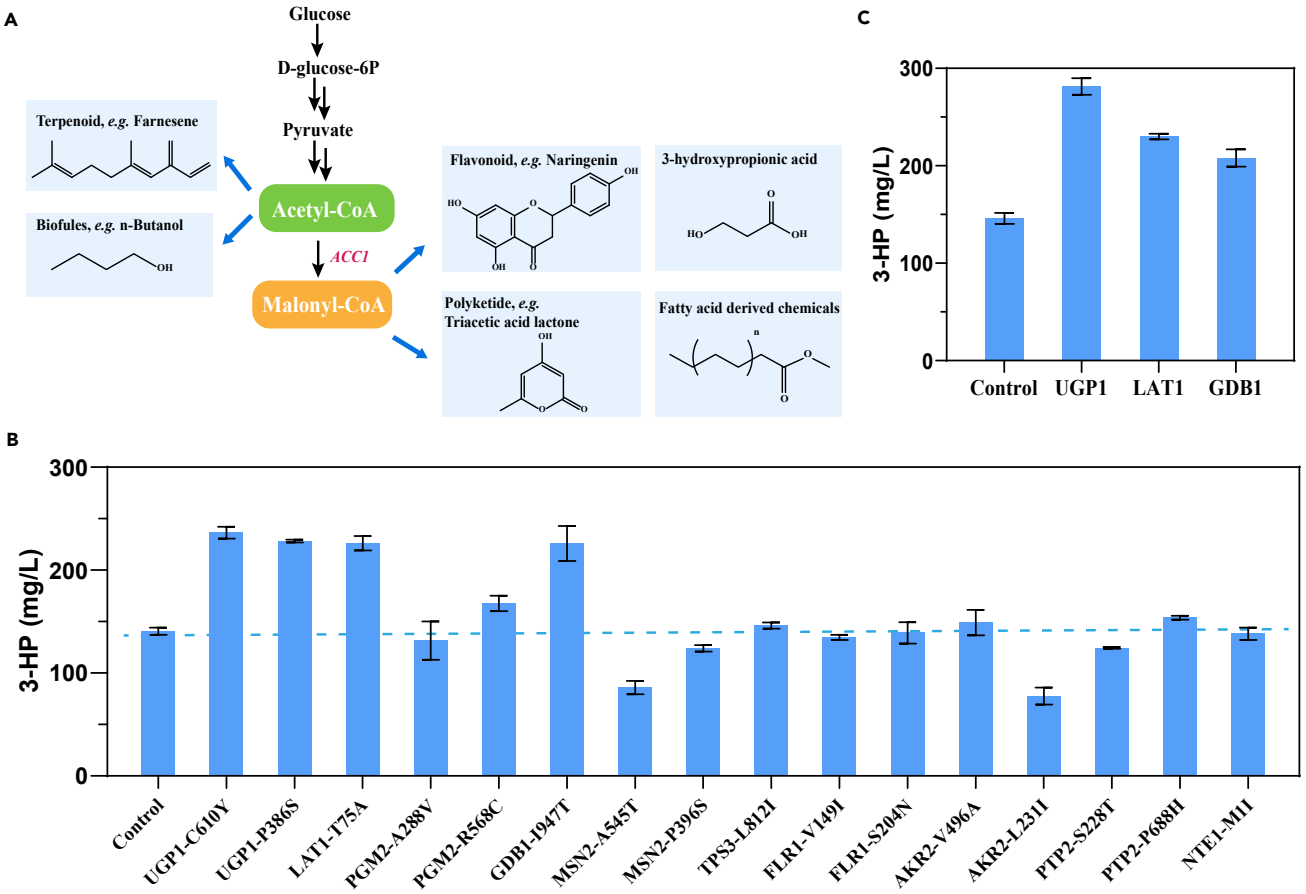

Figure 1. Identification of the causal genes for improving malonyl-CoA availability

(A) Overview of acetyl-CoA- and malonyl-CoA-derived chemicals.

(B) 3-HP production in the strains overexpressing the mutated genes isolated from genomic sequencing.

(C) 3-HP production in the strains overexpressing original *UGP1*, *LAT1*, and *GDB1*. The control strain is CEN.PK2-1C expressing pJFE3 plasmid. Data are represented as mean ± SD (n = 3, number of experiments). The statistically significant changes were determined by a two-tailed homoscedastic (equal variance) t-test and indicated by * if $p < 0.05$ or ** if $p < 0.01$.

storage carbohydrate synthesis.[22–25] Therefore, in this study, we analyzed how *UGP1* overexpression improves the malonyl-CoA level and demonstrated its role as a carbon buffer to regulate storage carbohydrate synthesis in different stages dynamically.

RESULTS

Overexpressing *UGP1*, *GDB1*, and *LAT1* genes improve the malonyl-CoA flux

Our previous study screened four mutant strains with improved malonyl-CoA flux using *in vivo* mutagenesis combined with a biosensor-mediated growth-based screening system. The commonly changed genes with single nucleotide polymorphisms (SNPs) and insertions-deletions (InDels) were identified by whole-genome sequencing.[18] Here, we overexpressed the commonly changed genes with SNPs in the control strain and then determined the production of a malonyl-CoA downstream chemical 3-HP by expression of malonyl-CoA reductase (MCR) in these strains. Interestingly, we found that overexpression of the mutant versions of *UGP1*, *LAT1*, and *GDB1* increases the 3-HP production by 40%–50% (Figure 1B). To determine whether the mutation or the expression level causes the increased production, the original *UGP1*, *LAT1*, and *GDB1* genes were overexpressed and 3-HP production also was increased (Figure 1C). Among them, *UGP1* overexpression shows the highest increase (73%) ($p < 0.01$). On the contrary, *in situ* mutations of these genes ($UGP1^{I484M}$, $UGP1^{P386S}$, $LAT1^{T47A}$, and $GDB1^{I947T}$) in the genome did not significantly increase 3-HP production.[18] Taken together, it can be concluded that the expression level, not the mutation, of these genes affects the malonyl-CoA flux.

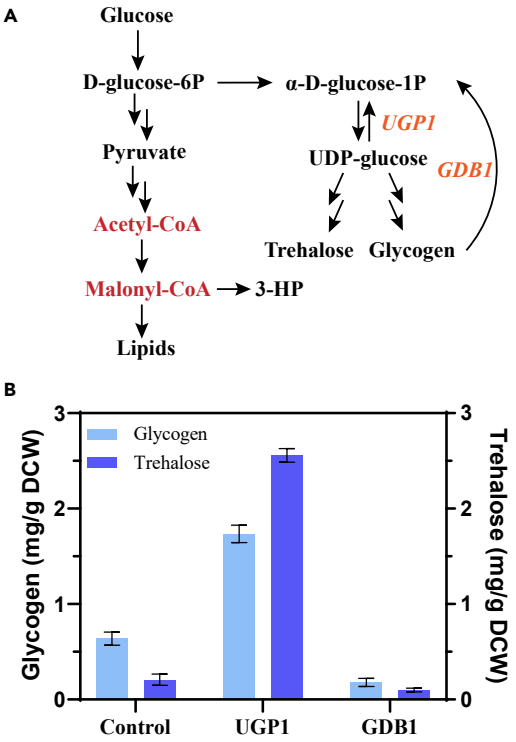

Figure 2. *UGP1* and *GDB1* overexpression affects glycogen and trehalose production

(A) The metabolic pathway of malonyl-CoA synthesis and glycogen and trehalose synthesis.

(B) The glycogen and trehalose production in the early exponential phase in *UGP1*- and *GDB1*-overexpressing strains and the control strain. The control strain is CEN.PK2-1C expressing the pJFE3 plasmid. Data are represented as mean ± SD (n = 3, number of experiments).

Lat1 is the dihydrolipoamide acetyltransferase component of the pyruvate dehydrogenase complex (PDH), which catalyzes the oxidative decarboxylation of pyruvate to acetyl-CoA.[26] Overexpression of *LAT1* may enhance the synthesis of acetyl-CoA in mitochondria and contribute to the cycle of carbon metabolism. Gdb1 is a glycogen-debranching enzyme that participates in glycogen degradation (Teste et al., 2000) (Figure 2A). In *S. cerevisiae*, glycogen is normally catabolized into glucose-1-phosphate and glucose, catalyzed by glycogen phosphorylase (Gph1p) and the Gdb1p debranching enzyme.[20] Ugp1 is a UDP-glucose pyrophosphorylase (UGPase) that catalyzes the reversible formation of UDP-glucose from glucose-1-phosphate and UTP for the biosynthesis of structural carbohydrates[23,27] such as β-glucans and storage carbohydrates (Figure 2A).[22,23]

Interestingly, we found that both *UGP1* and *GDB1* are associated with the synthesis and metabolism of storage carbohydrates. To further investigate the relationship between storage carbohydrates synthesis and malonyl-CoA availability, the glycogen and trehalose accumulation was determined (Figure 2B). Overexpression of *GDB1* decreases glycogen and trehalose synthesis. It seems that Gdb1 reduces the carbon flux to storage carbohydrates, thereby increasing the malonyl-CoA flux. This result is consistent with our previous work, in which we found that *PGM3* deletion increases 3-HP production and decreases glycogen accumulation.[18] However, in contrast to overexpressing *GDB1*, *UGP1* overexpression increases glycogen and trehalose accumulation and improves the 3-HP production. The 3-HP titer is found to be even higher than that in the *GDB1*-overexpressing strain. Therefore, it is necessary to investigate how Ugp1 affects the distribution of carbon metabolism.

Ugp1 dynamically regulates the carbon distribution between storage carbohydrates and glycolysis in different growth stages

Ugp1, a UGPase, catalyzes the reversible formation of UDP-glucose. UDP-glucose is used as a glucosyl donor in several cellular processes, including the synthesis of glycogen and trehalose,[22–24] β-glucan,[23,27] glycolipids and glycoproteins,[28,29] and galactose entry into glycolysis.[30] We systematically analyzed the metabolism of the *UGP1*-overexpressing strain and the control strain to investigate how the *UGP1*-overexpressing strain affected the malonyl-CoA flux. Compared with the control strain, the *UGP1*-overexpressing strain shows a lower growth rate and a lower glucose-consumption rate (Figures 3A and 3B). The production of glycogen and trehalose in different cultivation times was determined (Figures 3C and 3D). Interestingly,

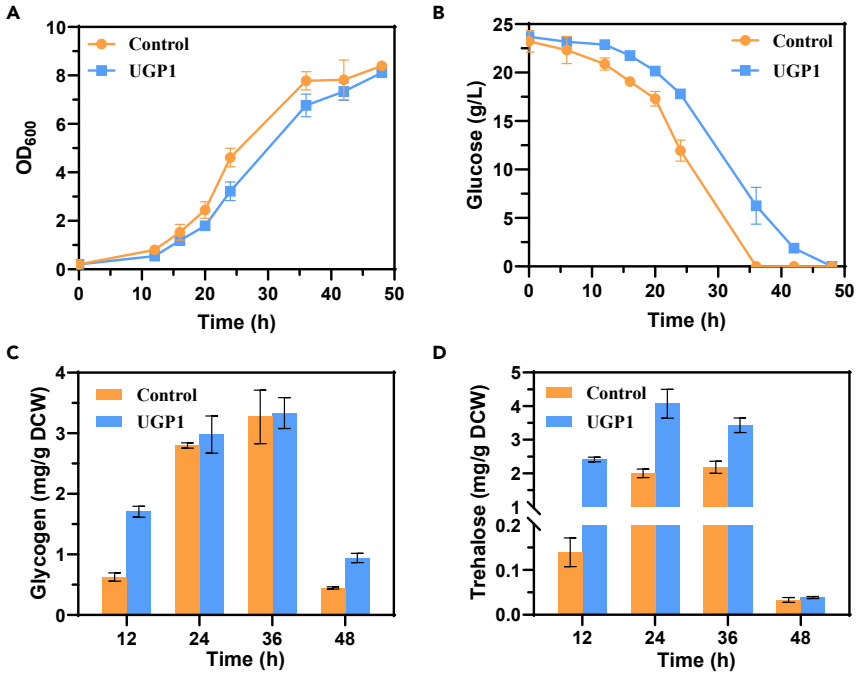

Figure 3. The effect of overexpression of *UGP1* on carbon metabolism and cell growth

(A–D) The cell growth (A) and glucose consumption (B) of the strain UGP1 and control strain. The glycogen (C) and trehalose (D) content in the early exponential phase, mid-exponential phase, and stationary phase in UGP1 and control strain. The control strain is CEN.PK2-1C expressing the pJFE3 plasmid. Data are represented as mean ± SD (n = 3, number of experiments).

although glycogen and trehalose accumulation in the *UGP1*-overexpressing strain is generally higher than in the control strain, their differences are more significant in the early exponential phase (at 12 h) than in the later phase. For example, in the early exponential phase, glycogen and trehalose levels in the *UGP1*-overexpressing strain are 1.7-fold and 2.3-fold higher than in the control strain, respectively. However, in the mid and late exponential phases (at 24 h and 36 h), although the levels of glycogen and trehalose are higher than in the early exponential phase in both strains, the differences between the two strains were reduced. The glycogen level is similar in both strains, and the trehalose accumulation in the *UGP1*-overexpressing strain is only 98% and 54% higher than that in the control strain at 24 and 36 h, respectively. Moreover, in the later phase (at 48 h), when glucose is fully consumed, glycogen and trehalose are reduced to a very low level, and the differences between the two strains are also relatively small (Figure 3D).

Conversely, the 3-HP production in the *UGP1*-overexpressing strain is lower than that in the control strain in the early exponential phase but higher in the later phase (Figure 4A). To monitor the malonyl-CoA level in real time, we introduced a malonyl-CoA biosensor (FapR/*TEF1up-fapOGAL1pcore-GFP*) in the *UGP1*-overexpressing and control strains. We have previously demonstrated that the malonyl-CoA level is positively correlated with the expression of GFP (Figure 4B).[31] Consistent with 3-HP production, the malonyl-CoA level of the *UGP1*-overexpressing strain is also lower in the early exponential phase but increases progressively in the later phase (Figure 4C). This means that overexpression of *UGP1* results in higher malonyl-CoA levels than in the control strain in the later phase. Storage carbohydrates have been considered carbon reservoirs for maintaining cells' carbon and energy charge.[20] It seems that *UGP1* overexpression results in a buffer effect that dynamically regulates the carbon flux. When glucose is in excess, the carbon flows to glycogen for carbon storage, and when the glucose level is low, the storage carbohydrates are consumed, and hence more carbon can be used to synthesize malonyl-CoA (Figure 4D).

UGP1 overexpression improves acetyl-CoA-derived-chemicals

Malonyl-CoA is synthesized from acetyl-CoA, which is generated from the decarboxylation of pyruvate to produce ethanol and acetate in *S. cerevisiae*.[8] Acetate is then catalyzed by acetyl-CoA synthase (ACS) to

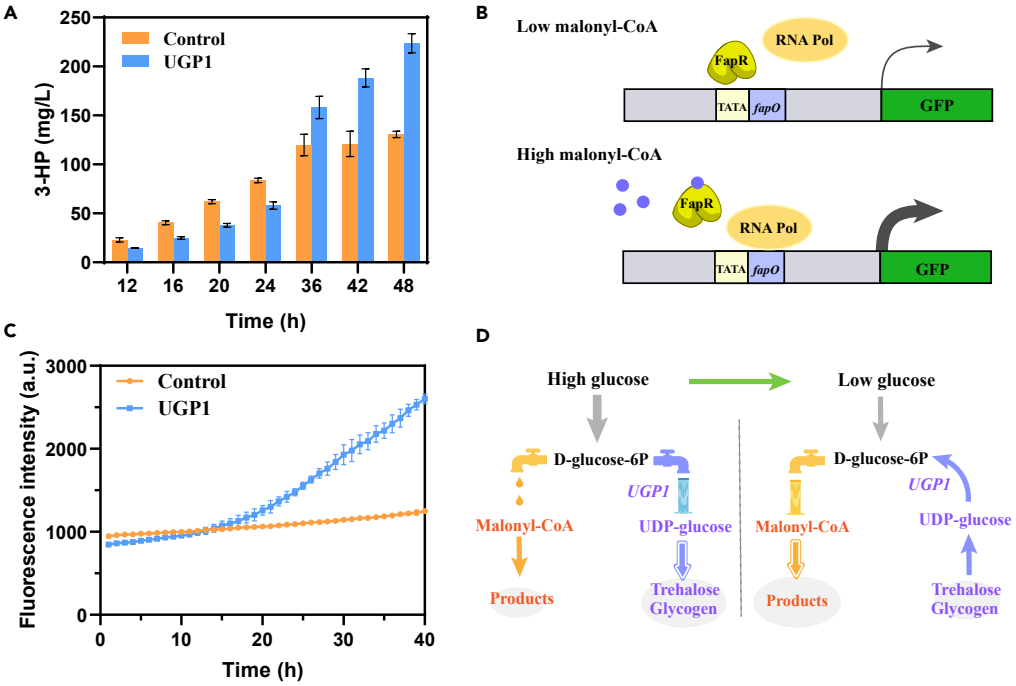

Figure 4. Effect of overexpressing *UGP1* on *GFP* expression driven by malonyl-CoA biosensor and 3-HP production

(A) 3-HP production of UGP1 and control strain in different cultivation times.

(B) Schematic diagram of the malonyl-CoA biosensor. When the intracellular malonyl-CoA level is low, FapR binds to the promoter and blocks the expression of GFP; when the intracellular malonyl-CoA level is high, FapR dissociates from the promoter and activates GFP expression.

(C) Fluorescence intensities of UGP1 and control strains expressing malonyl-CoA biosensor. (D) Schematic diagram of dynamically-tuning yeast storage carbohydrate to improve the production of acetyl-CoA derived chemicals. The control strain is CEN.PK2-1C expressing the pJFE3 plasmid. Data are represented as mean ± SD (n = 3, number of experiments).

produce acetyl-CoA. To determine whether *UGP1* overexpression also affects inherent yeast metabolites and acetyl-CoA metabolism, we then determined the production of acetate and ethanol and also detected an acetyl-CoA-derived chemical α-farnesene. The *UGP1* gene is expressed under the control of constitutive promoters with different strengths. Compared with the control strain, the strains with higher *UGP1* expression have lower growth rates and glucose consumption (Figures S1A and S1B) (Table 1). Ethanol and acetate production is also slower, indicating that overexpressing *UGP1* slows down byproduct synthesis by directing more carbon to storage carbohydrates. (Figures S1C and S1D) (Table 1).

The production of 3-HP (malonyl-CoA-derived chemical) and α-farnesene (acetyl-CoA-derived chemical) was then measured by expressing MCR or α-farnesene synthase. The 3-HP production of the *UGP1*-overexpressing strains is low in the early stage but gradually increases in the later stage (Figure 5A). Higher *UGP1* expression leads to higher production. The production of 3-HP can be increased by 97% with high *UGP1* expression. Similarly, with an increase in the expression level of *UGP1*, the production of α-farnesene also gradually increases. The most significant improvement was about 77%, compared with the control

Table 1. The maximum specific growth rate, glucose-specific consumption rate, and ethanol production rate of control strain and UGP1-overexpressing strains driven by *CYC1*, *TEF1*, and *PGK1* promoters

	Control	*CYC1p-UGP1*	*TEF1p-UGP1*	*PGK1p-UGP1*
μ_{max} (h^{-1})	0.23 ± 0.00	0.20 ± 0.00	0.18 ± 0.00	0.13 ± 0.00
$r_{glucose}$ (g g^{-1} DCW h^{-1})	1.18 ± 0.06	1.05 ± 0.00	0.97 ± 0.06	0.76 ± 0.02
$r_{ethanol}$ (g g^{-1} DCW h^{-1})	0.49 ± 0.01	0.44 ± 0.03	0.42 ± 0.02	0.35 ± 0.02

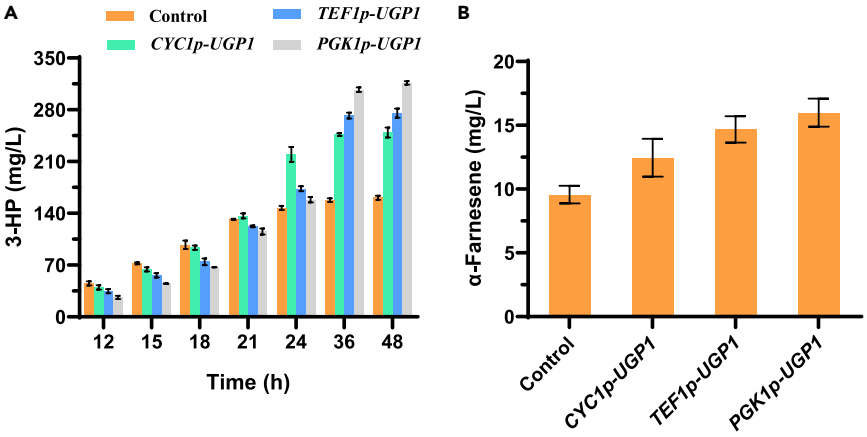

Figure 5. The synthesis of acetyl-CoA-derived products in *UGP1*-overexpressing strain

(A) 3-HP production of control strain and *UGP1*-overexpressing strains driven by *CYC1*, *TEF1*, and *PGK1* promoters expressing the pIY-mcr plasmid.

(B) α-farnesene production of control strain and *UGP1*-overexpressing strains driven by *CYC1*, *TEF1*, and *PGK1* promoters expressing the pIY-EGR20-FS plasmid. The control strain is CEN.PK2-1C expressing the pJFE3 plasmid. Data are represented as mean ± SD (n = 3, number of experiments). The statistically significant changes were determined by a two-tailed homoscedastic (equal variance) t-test and indicated by * if $p < 0.05$ or ** if $p < 0.01$.

See also Figure S1.

strain (Figure 5B) ($p < 0.05$). It is evident that higher *UGP1* expression has a better effect on carbon redistribution, thereby increasing the accumulation of acetyl-CoA and malonyl-CoA.

To verify whether *UGP1* overexpression can be combined with other casual genes that affect acetyl-CoA availability to increase chemical production further, we combined the *UGP1* overexpression with other genes that we identified and determined by 3-HP production (Figure 6) ($p < 0.01$). We found that the combination of different gene targets can further improve 3-HP production. For example, compared with *UGP1* single gene overexpression, the introduction of *SDH3* (the gene encoding subunit of succinate dehydrogenase) and the deletion of *ARG3* (the gene encoding ornithine carbamoyl transferase which is related to arginine synthesis) further increases 3-HP production by 50%. Therefore, our identified targets can be combined with other approaches to improve the production of acetyl-CoA- and malonyl-CoA-derived chemicals.

DISCUSSION

Storage carbohydrates are considered for usage in carbon reservoirs to maintain a yeast cell's energy charge.[21] Glucose is converted to storage carbohydrates to ensure sufficient material and energy are available for survival under stress and starvation conditions. Directly reducing glycogen and trehalose by overexpressing *GDB1* or *PGM3* deletion[18] facilitates the replenishment of carbon for malonyl-CoA synthesis. In this study, we demonstrated for the first time that dynamic-regulating storage carbohydrates by *UGP1* overexpression can also contribute to the synthesis of acetyl-CoA-derived chemicals. The effect is even more efficient than directly eliminating glycogen synthesis. Ugp1 catalyzes the biosynthesis of UDP-glucose, which is a precursor to carbohydrates and their derivatives and is considered a pivotal enzyme in glucose allocation.[23] Overproduction of UGPase increases the total amount of glycogen and trehalose.[23]

It directs more carbon flux to the synthesis of storage carbohydrates in the early exponential phase, thereby reducing the flow of glucose to the synthesis of ethanol and other metabolites and also reducing the cell growth slightly. When glucose concentration becomes low, it redirects the flux from storage carbohydrates to glycolysis, thereby allowing the cells to synthesize more acetyl-CoA/malonyl-CoA at a later phase, thus increasing the production of their respective derived chemicals.

Improving the availability of crucial metabolites in yeast remains challenging work due to being highly regulated by the metabolic network. In some cases, the co-overexpression of multiple target genes shows an antagonistic effect rather than a further enhancement of target production.[32] In this work, we found that combining *UGP1* with other selected gene targets can further enhance 3-HP production.

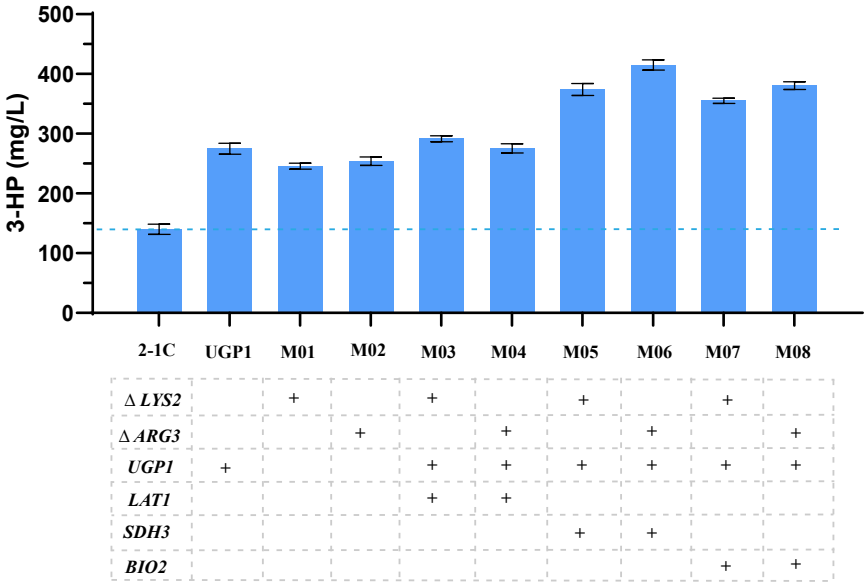

Figure 6. 3-HP production of overexpressing *LAT1-UGP1*, *SDH3-UGP1*, and *BI O 2-UPG1* in ΔLYS2 and ΔARG3 strains

Data are represented as mean ± SD (n = 3, number of experiments). The statistically significant changes were determined by a two-tailed homoscedastic (equal variance) t-test and indicated by ** if $p < 0.01$.

We believe that the new causal genes identified in our study will contribute to the synthesis of a broad range of acetyl-CoA-derived compounds.

Limitations of the study

In this study, we found that increasing the storage carbohydrate by *UGP1* overexpression improves metabolic fluxes toward malonyl-CoA- and acetyl-CoA-derived chemicals. Furthermore, we demonstrated that Ugp1 dynamically regulates carbon distribution between storage carbohydrates and glycolysis at different growth stages. However, we cannot exclude the possibility that it indirectly affects other metabolic pathways. The metabolic flux distribution will be measured in the future.

STAR★METHODS

Detailed methods are provided in the online version of this paper and include the following:

- KEY RESOURCES TABLE
- RESOURCE AVAILABILITY
  - Lead contact
  - Materials availability
  - Data and code availability
- EXPERIMENTAL MODEL AND SUBJECT DETAILS
  - Strains and growth media
- METHOD DETAILS
  - Media and culture conditions
  - Strains and plasmids construction
  - Glycogen and trehalose assays
  - Fluorescence intensity measurement
  - Metabolite analysis
- QUANTIFICATION AND STATISTICAL ANALYSIS
  - Statistical tests

SUPPLEMENTAL INFORMATION

Supplemental information can be found online at https://doi.org/10.1016/j.isci.2022.105817.

ACKNOWLEDGMENTS

This work was funded by the grants of National Key R&D Program of China (2019YFA0904900), the National Natural Science Foundation of China (31970082 and 31770101) and the National Natural Science Foundation of Shandong province (ZR2020YQ18 and ZR2022ZD24).

We thank Xiangmei Ren from the State Key laboratory of Microbial Technology of Shandong University for help and guidance in HPLC.

AUTHOR CONTRIBUTIONS

J.H. and Q.Q. designed the research. C.Q. and H.T. performed the experiments. C.Q., H.T., and J.H. analyzed the data. C.Q. and J.H. wrote the manuscript. All the authors edited the manuscript.

DECLARATION OF INTERESTS

The authors declare no competing interests.

Received: September 27, 2022
Revised: October 21, 2022
Accepted: December 13, 2022
Published: January 20, 2023

REFERENCES

1. Huang, J., and Huang, S. (2022). Bioproduction of monoterpene indole alkaloids in a single cell factory. Eng. Microbiol. *2*, 100050. https://doi.org/10.1016/j.engmic.2022.100050.

2. Li, S., Zhang, Q., Wang, J., Liu, Y., Zhao, Y., and Deng, Y. (2021). Recent progress in metabolic engineering of *Saccharomyces cerevisiae* for the production of malonyl-CoA derivatives. J. Biotechnol. *325*, 83–90. https://doi.org/10.1016/j.jbiotec.2020.11.014.

3. Nielsen, J. (2014). Synthetic biology for engineering acetyl coenzyme A metabolism in yeast. mBio *5*, e02153. https://doi.org/10.1128/mBio.02153-14.

4. Lian, J., Si, T., Nair, N.U., and Zhao, H. (2014). Design and construction of acetyl-CoA overproducing *Saccharomyces cerevisiae* strains. Metab. Eng. *24*, 139–149. https://doi.org/10.1016/j.ymben.2014.05.010.

5. Gong, G., Wu, B., liu, L., Li, J., Zhu, Q., He, M., and Hu, G. (2022). Metabolic engineering using acetate as a promising building block for the production of bio-based chemicals. Eng. Microbiol. *2*, 100036. https://doi.org/10.1016/j.engmic.2022.100036.

6. Tippmann, S., Ferreira, R., Siewers, V., Nielsen, J., and Chen, Y. (2017). Effects of acetoacetyl-CoA synthase expression on production of farnesene in *Saccharomyces cerevisiae*. J. Ind. Microbiol. Biotechnol. *44*, 911–922. https://doi.org/10.1007/s10295-017-1911-6.

7. Wang, J., Jiang, W., Liang, C., Zhu, L., Li, Y., Mo, Q., Xu, S., Chu, A., Zhang, L., Ding, Z., and Shi, G. (2021). Overproduction of α-farnesene in *Saccharomyces cerevisiae* by farnesene synthase screening and metabolic engineering. J. Agric. Food Chem. *69*, 3103–3113. https://doi.org/10.1021/acs.jafc.1c00008.

8. Chen, Y., Daviet, L., Schalk, M., Siewers, V., and Nielsen, J. (2013). Establishing a platform cell factory through engineering of yeast acetyl-CoA metabolism. Metab. Eng. *15*, 48–54. https://doi.org/10.1016/j.ymben.2012.11.002.

9. Gao, Q., Deng, S., Jiang, T., and Jiang, T. (2022). Recent developments in the identification and biosynthesis of antitumor drugs derived from microorganisms. Eng. Microbiol. *2*, 100047. https://doi.org/10.1016/j.engmic.2022.100047.

10. Saunders, L.P., Bowman, M.J., Mertens, J.A., Da Silva, N.A., and Hector, R.E. (2015). Triacetic acid lactone production in industrial *Saccharomyces* yeast strains. J. Ind. Microbiol. Biotechnol. *42*, 711–721. https://doi.org/10.1007/s10295-015-1596-7.

11. Wattanachaisaereekul, S., Lantz, A.E., Nielsen, M.L., and Nielsen, J. (2008). Production of the polyketide 6-MSA in yeast engineered for increased malonyl-CoA supply. Metab. Eng. *10*, 246–254. https://doi.org/10.1016/j.ymben.2008.04.005.

12. Rodriguez, A., Strucko, T., Stahlhut, S.G., Kristensen, M., Svenssen, D.K., Forster, J., Nielsen, J., and Borodina, I. (2017). Metabolic engineering of yeast for fermentative production of flavonoids. Bioresour. Technol. *245*, 1645–1654. https://doi.org/10.1016/j.biortech.2017.06.043.

13. Wang, Y., Chen, H., and Yu, O. (2014). A plant malonyl-CoA synthetase enhances lipid content and polyketide yield in yeast cells. Appl. Microbiol. Biotechnol. *98*, 5435–5447. https://doi.org/10.1007/s00253-014-5612-z.

14. Zhang, Q., Yu, S., Lyu, Y., Zeng, W., and Zhou, J. (2021). Systematically engineered fatty acid catabolite pathway for the production of (2S)-naringenin in *Saccharomyces cerevisiae*. ACS Synth. Biol. *10*, 1166–1175. https://doi.org/10.1021/acssynbio.1c00002.

15. Chen, Y., Bao, J., Kim, I.K., Siewers, V., and Nielsen, J. (2014). Coupled incremental precursor and co-factor supply improves 3-hydroxypropionic acid production in *Saccharomyces cerevisiae*. Metab. Eng. *22*, 104–109. https://doi.org/10.1016/j.ymben.2014.01.005.

16. David, F., Nielsen, J., and Siewers, V. (2016). Flux control at the malonyl-CoA node through hierarchical dynamic pathway regulation in *Saccharomyces cerevisiae*. ACS Synth. Biol. *5*, 224–233. https://doi.org/10.1021/acssynbio.5b00161.

17. Liu, C., Ding, Y., Zhang, R., Liu, H., Xian, M., and Zhao, G. (2016). Functional balance between enzymes in malonyl-CoA pathway for 3-hydroxypropionate biosynthesis. Metab. Eng. *34*, 104–111. https://doi.org/10.1016/j.ymben.2016.01.001.

18. Qiu, C., Huang, M., Hou, Y., Tao, H., Zhao, J., Shen, Y., Bao, X., Qi, Q., and Hou, J. (2022). Biosensor-coupled *in vivo* mutagenesis and omics analysis reveals reduced lysine and arginine synthesis to improve malonyl-coenzyme A flux in *Saccharomyces cerevisiae*. mSystems *7*, e0136621. https://doi.org/10.1128/msystems.01366-21.

19. Cardenas, J., and Da Silva, N.A. (2014). Metabolic engineering of *Saccharomyces cerevisiae* for the production of triacetic acid lactone. Metab. Eng. *25*, 194–203. https://doi.org/10.1016/j.ymben.2014.07.008.

20. François, J., and Parrou, J.L. (2001). Reserve carbohydrates metabolism in the yeast *Saccharomyces cerevisiae*. FEMS Microbiol. Rev. *25*, 125–145. https://doi.org/10.1111/j.1574-6976.2001.tb00574.x.

21. Wilson, W.A., Roach, P.J., Montero, M., Baroja-Fernández, E., Muñoz, F.J., Eydallin, G., Viale, A.M., and Pozueta-Romero, J. (2010). Regulation of glycogen metabolism in yeast and bacteria. FEMS Microbiol. Rev. *34*, 952–985. https://doi.org/10.1111/j.1574-6976.2010.00220.x.

22. Daran, J.M., Bell, W., and François, J. (1997). Physiological and morphological effects of genetic alterations leading to a reduced synthesis of UDP-glucose in *Saccharomyces cerevisiae*. FEMS Microbiol. Lett. *153*, 89–96. https://doi.org/10.1111/j.1574-6968.1997.tb10468.x.

23. Daran, J.M., Dallies, N., Thines-Sempoux, D., Paquet, V., and François, J. (1995). Genetic and biochemical characterization of the *UGP1* gene encoding the UDP-glucose pyrophosphorylase from *Saccharomyces cerevisiae*. Eur. J. Biochem. *233*, 520–530. https://doi.org/10.1111/j.1432-1033.1995.520_2.x.

24. Hedegaard, J., Horn, P., Lametsch, R., Søndergaard Møller, H., Roepstorff, P., Bendixen, C., and Bendixen, E. (2004). UDP-glucose pyrophosphorylase is upregulated in carriers of the porcine RN- mutation in the AMP-activated protein kinase. Proteomics *4*, 2448–2454. https://doi.org/10.1002/pmic.200300761.

25. Yi, D.G., and Huh, W.K. (2015). UDP-glucose pyrophosphorylase Ugp1 is involved in oxidative stress response and long-term survival during stationary phase in *Saccharomyces cerevisiae*. Biochem. Biophys. Res. Commun. *467*, 657–663. https://doi.org/10.1016/j.bbrc.2015.10.090.

26. Niu, X.D., Browning, K.S., Behal, R.H., and Reed, L.J. (1988). Cloning and nucleotide sequence of the gene for dihydrolipoamide acetyltransferase from *Saccharomyces cerevisiae*. Proc. Natl. Acad. Sci. USA *85*, 7546–7550. https://doi.org/10.1073/pnas.85.20.7546.

27. Delmer, D.P. (1999). CELLULOSE BIOSYNTHESIS: exciting times for A difficult field of study. Annu. Rev. Plant Physiol. Plant Mol. Biol. *50*, 245–276. https://doi.org/10.1146/annurev.arplant.50.1.245.

28. Herscovics, A., and Orlean, P. (1993). Glycoprotein biosynthesis in yeast. FASEB J. *7*, 540–550. https://doi.org/10.1096/fasebj.7.6.8472892.

29. Sandhoff, K., van Echten, G., Schröder, M., Schnabel, D., and Suzuki, K. (1992). Metabolism of glycolipids: the role of glycolipid-binding proteins in the function and pathobiochemistry of lysosomes. Biochem. Soc. Trans. *20*, 695–699. https://doi.org/10.1042/bst0200695.

30. Frey, P.A. (1996). The Leloir pathway: a mechanistic imperative for three enzymes to change the stereochemical configuration of a single carbon in galactose. FASEB J. *10*, 461–470.

31. Chen, X., Yang, X., Shen, Y., Hou, J., and Bao, X. (2018). Screening phosphorylation site mutations in yeast acetyl-CoA carboxylase using malonyl-CoA sensor to improve malonyl-CoA-derived product. Front. Microbiol. *9*, 47. https://doi.org/10.3389/fmicb.2018.00047.

32. Li, S., Si, T., Wang, M., and Zhao, H. (2015). Development of a synthetic malonyl-CoA sensor in *Saccharomyces cerevisiae* for intracellular metabolite monitoring and genetic screening. ACS Synth. Biol. *4*, 1308–1315. https://doi.org/10.1021/acssynbio.5b00069.

33. Gietz, R.D., and Woods, R.A. (2002). Transformation of yeast by lithium acetate/single-stranded carrier DNA/polyethylene glycol method. Methods Enzymol. *350*, 87–96. https://doi.org/10.1016/s0076-6879(02)50957-5.

STAR★METHODS

KEY RESOURCES TABLE

REAGENT or RESOURCE	SOURCE	IDENTIFIER
Bacterial and virus strains		
DH5α	TransGen Biotech	CD201-01
Chemicals, peptides, and recombinant proteins		
Amyloglucosidase	Sigma-Aldrich	CAS: 9032-08-0 Cat#A9228
Trehalase	Sigma-Aldrich	CAS: 9025-52-9 Cat#T8778
T4 DNA ligase	Thermo scientific	Cat#EL0011
3-Hydroxypropionic acid	Aladdin	CAS:6149-41-3
α- Farnesene	ABPHYTO	CAS No.: 502-61-4
Critical commercial assays		
Glucose Colorimetric/Fluorometric assay kit	Sigma-Aldrich	Cat#MAK263
Gibson Assembly mix	New England Biolabs	E2611
Deposited data		
The whole-genome-Seq Raw data	GenBank	PRJNA750225
Experimental models: Organisms/strains		
S. cerevisiae, strain background: CEN.PK2-1C	EUROSCARF	http://www.euroscarf.de/index.php?nameNews
Oligonucleotides		
For all PCR Primers, see Table S1	This paper	N/A
Recombinant DNA		
For all plasmids, see Table S2	This paper	N/A
Software and algorithms		
Prism (Version 8.0.1)	GraphPad	N/A

RESOURCE AVAILABILITY

Lead contact

Further information and requests for resources and reagents should be directed to and will be fulfilled by the lead contact, Jin Hou (houjin@sdu.edu.cn).

Materials availability

This study did not generate new unique reagents.

Data and code availability

- This paper analyzes existing, publicly available data. The accession numbers for the datasets are listed in the key resources table.
- This paper does not report the original code.
- Any additional information required to reanalyze the data reported in this paper is available from the lead contact upon request.

EXPERIMENTAL MODEL AND SUBJECT DETAILS

Strains and growth media

The yeast strains used in this study were derived from ***S. cerevisiae*** CEN.PK 2-1C (*MATa; ura3-52; trp1-289; leu2-3,112; his3Δ1; MAL2-8C; SUC2*). Standard methods for yeast culture, gene disruption, and transformation were applied. The strains used in this study were listed in Table S3.

METHOD DETAILS

Media and culture conditions

Escherichia coli strain DH5α was used for recombinant DNA manipulation and was cultivated in Luria-Bertani (LB) broth (5 g/L yeast extract, 10 g/L tryptone, and 10 g/L NaCl) at 37°C in shake flasks with a shaking speed of 200 rpm. LB was supplemented with 100 mg/L ampicillin for plasmid maintenance and propagation.

Yeast strains were grown in YPD medium or Synthetic complete (SC) dropout medium at 30°C according to the auxotrophy of the cells. YPD medium containing 10 g/L yeast extract, and 20 g/L peptones, supplemented with 20 g/L glucose, was used to culture yeast cells without any plasmid. For 3-HP production in falcon tubes or shake flasks, *S. cerevisiae* strains were cultured for 48 h at 200 rpm shaking, 30°C in the SC dropout media. The media comprised 1.7 g/L yeast nitrogen base without amino acids (BBI Life Science Corporation, China), 5 g/L ammonium sulfate, SC drop-out medium without uracil, leucine and/or histidine (Sunrise Science Products, San Diego, CA, USA), and 20 g/L glucose. When necessary, 60 mg/L leucine (BBI Life Science Corporation, China), or 20 mg/L uracil (BBI Life Science Corporation, China) was added to the growth medium.

Strains and plasmids construction

All strains and plasmids used and constructed in this study are listed in Table S2 and S3, respectively. All primers used in this study are listed in Table S1. Plasmids were constructed by restriction enzyme digestion and ligation or Gibson assembly.

S. cerevisiae CEN.PK 2-1C (MATa; ura3-52; trp1-289; leu2-3,112; his3Δ1; MAL2-8C; SUC2) was used as the background strain for all the experiments. For constructing over-expression plasmids, the gene fragment was amplified from the genome of CEN.PK 2-1C or mutant strains by corresponding primer pairs. The DNA fragments were digested with restriction enzymes and ligated into the expression vector pJFE3. To construct different expression levels of *UGP1*, it is constructed under the control of *PGK1p*, *TEF1p*, and *CYC1p* and cloned into the multi-copy plasmid, pJFE3. To construct cover-expression plasmids, the *BI O 2*, *LAT1* or *SDH3* was assembled with the *TEF1* promoter and the *TEF1* terminator into the pJFE3 plasmid to yield pJ-BIO2, pJ-LAT1, pJ-SDH3; and the *UGP1* was assembled with the *PGK1* promoter and the *CYC1* terminator into the pJ-BIO2, pJ-LAT1, or pJ-SDH3 plasmid to yield pJ-BIO2-UGP1, pJ-LAT1-UGP1, pJ-SDH3-UGP1, respectively. The standard chemical transformation LiAc/PEG method was used for yeast transformation.[33]

Glycogen and trehalose assays

Yeast cultures were grown and harvested at different times, and approximately 100 OD_{600} of culture was harvested and washed twice with sterile H_2O. The pellets were collected and frozen in liquid nitrogen. The pellets were resuspended in 500 μL of 0.25 M Na_2CO_3 and incubated for 4 h at 95°C, followed by the addition of 0.15 mL of 1 M acetic acid and 0.65 mL of 0.2 M sodium acetate (pH 5.2) to the sample. Glycogen was digested by 70 U/mg amyloglucosidase (10115, Sigma-Aldrich) overnight at 57 °C. Trehalose was digested by 0.05 U/mL trehalase (T8778, Sigma-Aldrich) overnight at 37 °C under constant shaking. After digestion, the supernatants were collected and the glucose concentration derived from glycogen or trehalose was measured using the Glucose Colorimetric/Fluorometric assay kit (MAK263, Sigma-Aldrich).

Fluorescence intensity measurement

Fluorescence intensity was measured with a Multi-Detection Microplate Reader (Synergy HT, BioTtek, Winooski, VT, USA). Cell density was measured at 600 nm and the excitation and emission wavelengths for GFP were 485 ± 20 and 585 ± 20 nm, respectively. To measure the fluorescence of the UGP1 *over-expressing and control strains, an overnight culture was collected, inoculated into fresh SC media with an initial* OD_{600} *of 0.2, and cultivated for 48 h.*

Metabolite analysis

Strains were pre-cultured in tubes with 5 mL of SC medium. Seed cultures were inoculated into shake flasks with a working volume of 40 mL and an initial OD_{600} of 0.2 for 48 h. For the extraction of α-farnesene, 10% (v/v) dodecane was added to the medium. The concentrations of 3-HP and glucose were measured by HPLC

(Shimadzu Corporation, Japan) equipped with an Aminex HPX-87H column (Bio-Rad, Hercules, CA, USA). For analysis of glucose, ethanol, and acetic, the HPLC system was run at 45°C with 5 mM H_2SO_4 as mobile phase at a flow rate of 0.6 mL/min; and for analysis of 3-HP, H_2SO_4 (2.5 mM) was used as the mobile phase with a flow rate of 0.6 mL/min, and the temperature of the column was 65°C. The concentrations of α-farnesene were measured using a GC (Shimadzu Co., Kyoto, Japan) equipped with an Rtx-5 capillary column (30 m × 250 μm, i.d., 0.25-μm film thickness) and a flame ionization detector (FID). The temperatures of the injector and the detector were set at 280 and 290°C, respectively. The oven temperature was starting at 80°C for 1 min followed by heating the column to 250 °C at 10°C/min increase, and holding at 250 °C for 1 min, then to 280 °C at 10°C/min increase and held for 2 min.

QUANTIFICATION AND STATISTICAL ANALYSIS

Statistical tests

P-values were calculated using a two-tailed homoscedastic (equal variance) t-test in Prism GraphPad. Statistical details of the experiments can be found in the figure legends.